3

Panorama of gravitational-wave sources

Romano Joseph D[1]

[1] *Department of Physics and Astronomy*
University of Texas Rio Grande Valley
One West University Boulevard, Brownsville, TX 78520, USA

In this chapter, I give a brief, non-mathematical, "bird's eye view" of gravitational-wave sources across a broad range of source types, signal classes, and frequency bands. You will encounter these sources again, in much more detail, in several of the subsequent chapters.

3.1. Introduction

These notes provide a brief overview of various sources of gravitational waves (GWs). Since this is a broad introduction to the topic, I won't go into very much mathematical detail. You will get that detail in subsequent chapters from other instructors. Nonetheless, I believe it is useful to learn some of the basic vocabulary of GW sources and their corresponding signals early on, before diving into the heavy math.

In general, one can classify GW sources in terms of either: (i) the *physical objects or processes* that produce the GWs, or (ii) the *properties of the GW signals* that the sources produce in the detectors that we use to observe them. Being a data analyst, I often focus on the latter classification, asking what properties of the GW signals allow one to identify (and separate when necessary) the different sources.

GRAVITATIONAL WAVES,
coordinated by Nicola Tamanini (L2IT/CNRS).

This chapter is organized as follows: We start in Sec. 3.2 by discussing GW signal properties. We will restrict attention to *deterministic* signals and some of their sources in Sec. 3.3. After that, we will discuss *stochastic* GW signals and their sources, both astrophysical and cosmological in origin, in Sec. 3.4. Throughout this chapter, we will make reference to material from: (Allen and Romano 2023) (Allen 1997) (Christensen 2018) (Caprini and Figueroa 2018), and (Romano and Christensen 2025). Readers are recommended to visit these sources to obtain more details.

3.2. Signal properties

Let's start in the time domain, classifying the GW signals in terms of their duration, either short or long, relative to the observation time (typically, a year or so), and whether they have deterministic or non-deterministic waveforms. Short-duration signals are often called *transients*, while long-duration signals are said to be *persistent*. Deterministic waveforms have a "well-defined, predictable phase evolution", while non-deterministic (also known as stochastic or random) signals have a "non-predictable phase evolution".

With this classification, GW signals fall into one of four categories as shown in Fig. 3.1. An example of a short duration, deterministic signal is shown in the top left-hand panel, while an example of a long duration, non-deterministic signal is shown in the bottom right-hand panel. Possible sources for each of the signal classes are (moving clockwise, from upper left to bottom left): (i) A pair of black holes undergoing the final inspiral, merger, and ringdown to a single black hole; (ii) a rotating (non-axisymmetric) neutron star; (iii) a supernova explosion; (iv) a population of pairs of supermassive black holes orbiting one another in the centers of millions of merging galaxies.

Probably not surprisingly, the GW search groups in the LIGO-Virgo-KAGRA (LVK) Collaboration are divided precisely according to these signal or source classes. Following the same order as above, these are the Compact Binary Coalescence (CBC) Group, the Continuous Wave (CW) Group, the Unmodeled Burst Group, and the Stochastic Gravitational-Wave Background (SGWB) Group.

3.3. Deterministic signals

As mentioned above, deterministic signals have a well-defined, coherent phase evolution in the time domain. The simplest example of a deterministic signal is a sinusoid, like that shown in the top right-hand panel of Fig. 3.1. Another example of a deterministic signal is a GW *chirp*, which consists of oscillations that increases in amplitude and frequency over time until it reaches its

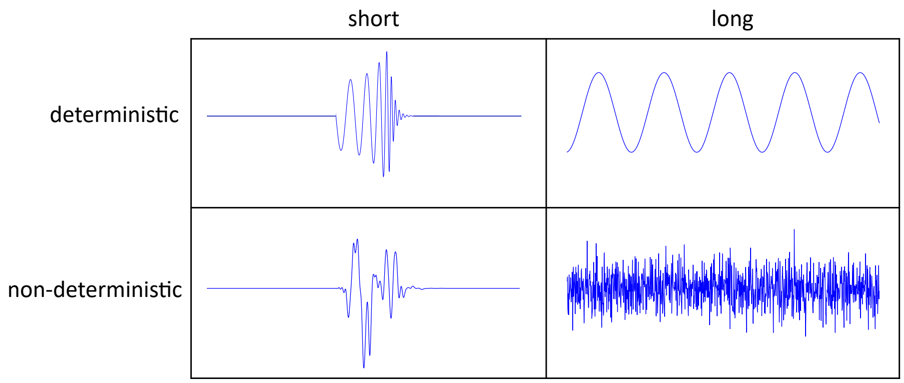

Figure 3.1: Classification of GW signals in terms of their duration (short or long) and phase evolution (deterministic or non-deterministic). Representative time-series data are shown for each class. [Credit: Adapted from Figure 4 in (Jenkins 2021).]

peak amplitude. It then decays like an exponentially damped sinusoid, like that shown in the top left-hand panel of Fig. 3.1. The following subsections go into more detail regarding possible sources for each of these types of deterministic signal.

3.3.1. *Continuous wave sources*

The simplest example of a CW source of GWs is a rotating non-axisymmetric neutron star (NS) with a "bump" on it, which lies somewhere off the rotational axis of the NS. Due to the "bump", the NS has a non-zero, timing-varying quadrupole moment, which is needed for the production of GWs. The frequency of the emitted GWs will equal twice the rotational frequency of the NS. The frequency of the signal will be approximately constant, changing only if the rotational frequency of the NS itself changes, or due to relative motion between the source and the detector (so-called Doppler modulation).

Another example of a CW source is the *early* inspiral of a binary system consisting of NSs or black holes (BHs). During the early inspiral phase (which can last millions of years), the GWs produced by the oribiting objects are approximately monochromatic (i.e., constant) over the timescale of an observation (typically years to decades). The frequency of the GWs does increase over time, since the orbital radius decreases due to energy radiated from the system in the form of GWs. But during the early inspiral phase, the change in frequency is much smaller than the width of an observational frequency bin ($\Delta f = 1/T_{\mathrm{obs}}$), so it is effectively a single-frequency signal.

A pair of supermassive BHs (having masses $\sim 10^9$ times the mass of the Sun) in the centers of two merging galaxies, emitting GWs in the frequency band 10^{-9} Hz – 10^{-7} Hz (relevant for pulsar timing arrays (PTAs)), is a concrete example of this last type of CW source. The SMBHB system slowly evolves for millions of years before it exits the PTA band and merges at a higher frequency.

3.3.2. *Compact binary coalescence*

The canonical source for a GW *chirp* is the late-stage inspiral, merger, and ringdown of a pair of NSs or BHs, or a NS-BH binary. This was the case for GW150914, which was the first direct observation of GWs by the LIGO GW detectors on 14 Sep 2015 (Abbott *et al.* 2016). The binary system that produced the GWs consisted of two BHs each having a mass roughly 30 times the mass of the Sun. Such an inspiral and merger event is called a *compact binary coalescence*.

The word "compact" here refers to the relatively small size of the coalescing objects. NSs, BHs, and white dwarfs (WDs) are all examples of compact objects. They are the three end states of stellar evolution. Low mass stars, having masses between $\sim$0.1 and 8 solar masses (one solar mass $M_\odot \approx 2\times 10^{30}$ kg) will end up as WDs. A WD has a mass $\sim 1.4 M_\odot$ and radius roughly equal to that of Earth. More massive stars, having masses between 8 and 25 $M_\odot$, eventually collapse to form a NS after a violent supernova explosion, which again has a mass roughly equal to 1 $M_\odot$ but with a radius $\sim$10 km (the size of a small city). Finally, stars with masses $\gtrsim 25 M_\odot$ evolve to form a BH. The masses of the BHs formed from stellar collapse range from about $5M_\odot$ to roughly $50M_\odot$. Black holes with masses $\gtrsim 50M_\odot$ can be formed from the collapse of very massive stars in the early universe (so-called Population-III stars), or from successive mergers of smaller-mass BHs. The characteristic size of a BH is given by its *Schwarzshild radius*, $R_s \equiv 2GM/c^2$, which is the radius of the event horizon of the black hole. (Here, G is Newton's gravitational constant, and c is the speed of light.) For reference, $R_s \approx 3$ km for $M = M_\odot$.

Primordial BHs (PBHs), which are created in the early Universe via the collapse of density perturbations of the primordial plasma, can have much smaller masses than BHs formed from the collapse of ordinary stars discussed above. But PBHs with masses $M \lesssim 10^{12}$ kg (which is the mass of a small asteroid) will have already evaporated due to Hawking radiation. The time needed for a BH to evaporate is $t_{\mathrm{evap}} \approx 10^{64}(M/M_\odot)^3$ yr.

Just like the relationship between the size of a musical instrument and the frequeny of the sound waves that it produces, so too do more massive gravitational systems produce lower-frequency GWs. For binary BHs (BBHs), there is a simple inverse relationship between the merger frequency of the binary system and its total mass M,

$$f_{\rm merger} = \frac{c^3}{6^{3/2}\pi GM}\,, \qquad [3.1]$$

which can be derived using Kepler's 3rd law $\omega^2 a^3 = GM$, where $\omega = 2\pi f_{\rm orb} = \pi f_{\rm merger}$, where $f_{\rm merger}$ is the GW frequency at $a = 6GM/c^2$, which is the radius of the innermost circular orbit for BBHs (so right before the merger). This is the highest GW frequency that the BBH system will produce. Figure 3.2 shows the frequency bands and different GW detectors needed to detect GWs from compact binary systems having different component masses.

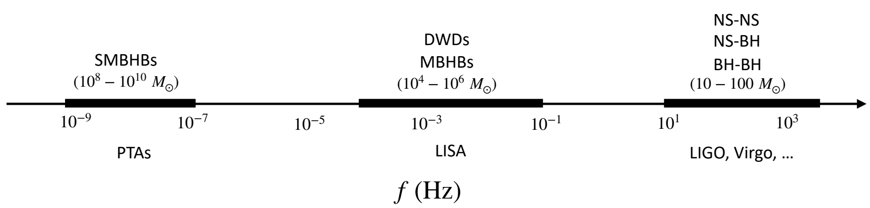

Figure 3.2: The frequency bands and detectors needed to detect GWs from compact binary systems having different masses.

NS / stellar-mass BH binaries: GW150914 was the first direct detection of GWs from the final inspiral and merger of two stellar-mass black holes (Abbott *et al.* 2016). Since that first observation on 14 Sep 2015, more than 100 additional binary black hole (BBH) mergers have been detected by the Advanced LIGO and Virgo detectors. All of these mergers have involved pairs of BHs having masses between 5 and 100 $M_\odot$, which is relevant for the frequency range (~10-1000 Hz) of the Advanced LIGO and Virgo detectors.

On 17 Aug 2017, the two Advanced LIGO detectors together with the European GW detector, Virgo, again detected GWs. But this time it was from the final inspiral and merger of two NSs (Abbott *et al.* 2017). This event, denoted GW170817, was the first *multi-messenger* observation of a GW event, being also observed in various forms of light across the electromagnetic spectrum. Since NSs are made of matter, when they smashed into one another after the final orbits of GW170817, electromagnetic radiation was produced in the process. In fact, some of the constituent neutrons were rapidly converted into heavier elements, most notably gold and platinum. It had long been conjectured that BNS mergers were the source of these heavy metals, but it wasn't until GW170817 that this conjecture could be confirmed.

As of the time of writing, there has been only one more confirmed detection of GWs from a BNS inspiral and merger, GW190425 (Abbott *et al.* 2020). Nonetheless, such BNS mergers are expected to be common throughout the Universe. Rate estimates predict roughly 1 BNS merger in the visible Universe every ~ 15 sec. On the other hand, stellar-mass BBH mergers are expected to occur every 5–10 minutes somewhere in the visible Universe.

White dwarf binaries: Galactic WD binaries (often denoted DWD for "double white dwarfs") are a prime source for the planned space-based detector LISA (Laser Interferometer Space Antenna). In fact, the combined "confusion noise" signal from millions of unresolved DWDs radiating in the LISA band (10^{-4} Hz to 10^{-1} Hz) will dominate the LISA instrumental noise at low frequencies, see Fig. 3.3. This stochastic GW *foreground* will act much like detector noise when trying to detect other GW signals with LISA.

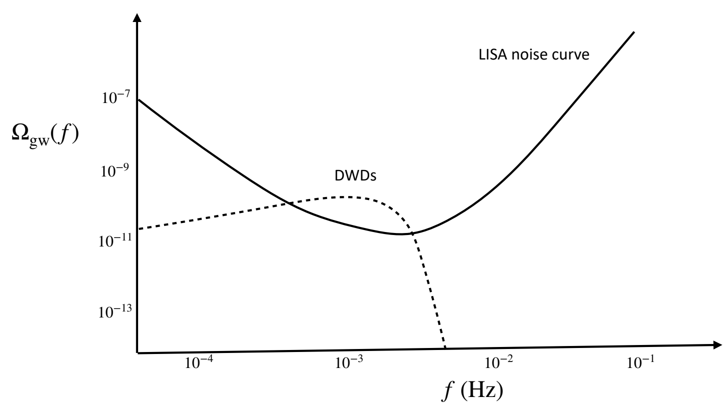

Figure 3.3: The confusion noise from the population of unresolved galactic white dwarf binaries. At low frequencies, this confusion noise exceeds the LISA instrumental noise. It is an example of an astrophysical foreground that must be contended with when searching for signals from other, weaker GW sources.

Loud individually resolvable DWDs can be seen above the above the unresolved background. One expects to be able to detect tens of thousands of such binaries over the four-year duration of LISA. Of these, approximately 20 DWDs have already been observed electromagnetically, so observing these system via the GWs that they also produce will be a good initial test of LISA. As such, these systems are often called LISA "verification binaries" in the literature.

Supermssive-black-hole binaries: SMBHBs are on the very-low-frequency end of the GW spectrum. Such systems are expected to form in the centers of merging galaxies, with the orbiting SMBHs producing GWs in the process. As mentioned earlier, SMBHBs with masses of order $10^9\ M_\odot$ will merge outside the PTA sensitivity band (10^{-9} Hz–10^{-7} Hz), at frequencies $\gtrsim 10^{-6}$ Hz. Thus, after entering the PTA band, the SMBHs will orbit one another for several million years before they coalesce, producing a monochromatic (CW) signal over the the timeframe of a typical observation (years to decades).

3.4. Stochastic signals and sources

Many different GW sources can give rise to a stochastic GW background. The only condition is that the GW signals that the sources produce should be individually unresolvable. This will be the case if the signals are either too weak or too numerous (interfering with one another in the time or frequency domain) to be individually detected. Since this statement depends on the sensitivity of the detectors, GW sources now that are currently unresolvable become resolvable, standing out above the lower levels of instrumental and environmental noise.

In the following subsections, we first discuss the signal properties of stochastic GWs. We then describe several different sources, of both astrophysical and cosmological origin.

3.4.1. *Signal properties*

Stochastic signals, being random, do not have deterministic (i.e., phase-coherent) waveforms. They look much like noise in a single detector. Examples of some very simple, simulated stochastic signals in the time domain are shown in Fig. 3.4 and as excess power coming from different directions on the sky in Fig. 3.5.

Let's start with Fig. 3.4. (i) The left-hand panel is the time-domain representation of a stochastic signal that is *continuous in time*. Since it is weaker than the noise, it is called a "background" signal. A possible source of this type of signal is the population of SMBHBs in the centers of merging galaxies throughout the visible Universe, each pair producing approximately monochromatic GWs which interfere with one another. (ii) The middle panel represents a

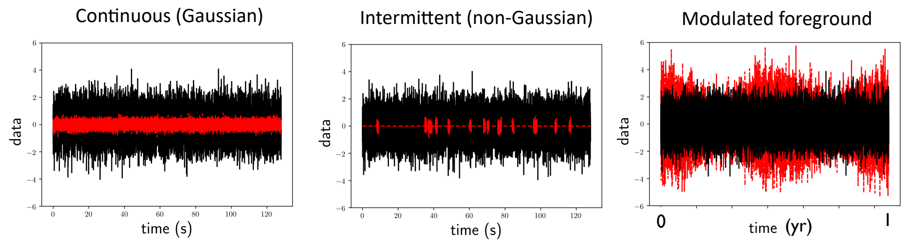

Figure 3.4: Simulated time-series data corresponding to different stochastic processes: (i) continuous-in-time, (ii) intermittent (or "popcorn-like"), and (iii) a modulated foreground. The red traces shows the GW signal; the black is simulated detector noise (assumed here to be white); and the vertical scales have arbitrary units.

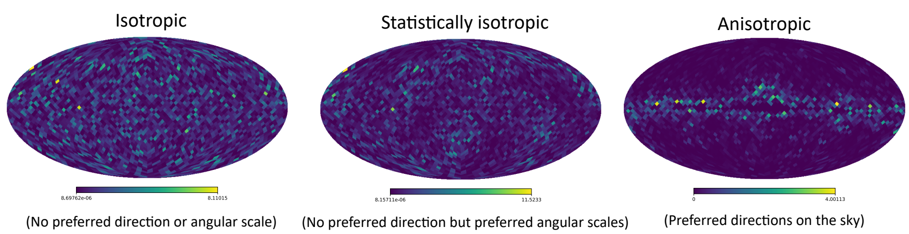

Figure 3.5: Example skymaps of GW power for (i) isotropic, (ii) statistically isotropic, and (iii) anisotropic source distributions. [Credit: Deepali Agarwal]

stochastic background signal that is *intermittent*, or "popcorn-like". A possible source for this type of signal is the population of stellar-mass BBHs, relevant for searches using the ground-based LVK detectors. The individuals merger signals are too weak to be individually detected; their durations ($\lesssim 1$ sec) are short relative to the average time between successive signals (∼5–10 minutes); and the arrival time of the individual signals are random (Poisson distributed). So the combined signal is stochastic, even though the individual BBH mergers are determinisic chirps. In contrast, the population of BNS mergers gives rise to a continuous-in-time stochastic background signal since the typical time in band for a BNS inspiral and merger is ~ 200 sec, while the average time between successive signals is only ~ 15 sec. (iii) The right-hand panel is an example of a "modulated foreground" stochastic signal, having a predictable time variation and being stronger than the noise. A possible source for this type of signal is the population of millions of DWDs in the Milky Way galaxy producing a "confusion-limited" foreground signal. The modulation is due to the orbital motion of the constellation of the three LISA spacecraft as it performs a "cartwheel" during its yearly motion around the Sun. As mentioned previously, the combined signal from these DWDs is so loud that it dominates the LISA noise at low frequencies (see Fig. 3.3).

The different panels of Fig. 3.5 correspond to skymaps of GW power on the sky for different GW source distributions. (i) The left-hand panel is for a purely *isotropic* signal. For this case, on average, there is no preferred direction on the sky, nor preferred angular scales for the distribution of GW power. (ii) The middle panel correspond to a *statistically-isotropic* signal, like that for the cosmic microwave background (CMB), which is a stochastic background of *electromagnetic* waves. Again, on average, there is no preferred direction of the GW power on the sky. But now there can be preferred angular scales. This is most easily seen by squinting your eyes at the middle panel, making it easier to see patches having different angular scales. (iii) The right-hand panel corresponds to a statistically *anisotropic* distribution of GW power on the sky, which traces the angular distribution of the GW sources giving rise to the signal. An example of a source that would produce such a skymap is the population of unresolved DWDs in the Milky Way, relevant for LISA, which we described in the context of Fig. 3.3. The excess GW power traces the shape of the Milky Way galaxy, seen in this skymap plotted in galactic coordinates.

3.4.2. *Characterization of stochastic signals in terms of power spectra*

Since stochastic signals do not have deterministic waveforms, they must be characterized instead in terms of their power spectra, their distribution on the sky (e.g., potential anisotropy), and / or the correlations they induce across multiple detectors. The power spectrum of a time-domain signal $h(t)$ is defined as

$$S_h(f) \equiv \frac{2}{T}\langle|\tilde{h}(f)|^2\rangle\,, \qquad [3.2]$$

where T denotes the duration of the data, $\tilde{h}(f) \equiv \int_{-\infty}^{\infty} \mathrm{d}t\; h(t)e^{-i2\pi ft}$ is the Fourier transform of $h(t)$, and angle brackets $\langle\;\rangle$ denotes an average over elements of an ensemble of possible universes, which can be thought of as draws from a probability distribution for a given set of parameters. If $h(t)$ has units of strain (which is dimensionless), then $S_h(f)$ is called the *strain power spectral density*, and has units of strain^2/Hz. The above definition of the power spectrum can be generalized to *cross spectra* $C_{12}(f) \equiv \frac{2}{T}\langle\tilde{h}_1(f)\tilde{h}_2^*(f)\rangle$, where $\tilde{h}_{1,2}(f)$ are the Fourier transforms of the response of two detectors to a GWB.

Isotropic stochastic backgrounds are typically characterized by the (dimensionless) *energy density spectrum*

$$\Omega_{\rm gw}(f) \equiv \frac{1}{\rho_{\rm crit}}\frac{{\rm d}\rho_{\rm gw}}{{\rm d}(\ln f)} = \frac{f}{\rho_{\rm crit}}\frac{{\rm d}\rho_{\rm gw}}{{\rm d}f}\,, \qquad [3.3]$$

where ${\rm d}\rho_{\rm gw}$ is the energy density in GWs contained in the frequency interval f to $f + {\rm d}f$, and $\rho_{\rm crit} \equiv 3H_0^2c^2/8\pi G$ is the critical energy density needed to close the universe today. Here, $H_0 \equiv \dot{a}(t)/a(t)|_{t=t_0}$ is the *Hubble expansion rate* evaluated today, and $a(t)$ is the *scale factor* describing the expansion of the Universe as a function of time. $\Omega_{\rm gw}(f)$ is related to the strain power spectrum $S_h(f)$ via

$$S_h(f) = \frac{3H_0^2}{2\pi^2}\frac{\Omega_{\rm gw}(f)}{f^3}\,. \qquad [3.4]$$

So its a simple matter to go back and forth between the power spectrum $S_h(f)$ and the energy density spectrum $\Omega_{\rm gw}(f)$ for a stochastic GW background.

3.4.3. *Astrophysical sources*

Astrophysical sources of a stochastic GW background are associated with *populations* of compact stars or stellar remnants which formed $\gtrsim 1$ billion years after the Big Bang. These populations include NS / stellar-mass BH binaries (relevant for ground-based detectors like LIGO, Virgo, KAGRA), DWDs (relevant for LISA), and SMBH binaries (relevant for PTAs), which we discussed previously in Sec. 3.3.2.

Using the definition of $\Omega_{\rm gw}(f)$ given in [3.3], one can show that for a population of inspiraling binaries, $\Omega_{\rm gw}(f) \propto f^{2/3}$. This result is a consequence of Kepler's third law $\omega^2 a^3 = {\rm const}$, the relationship between orbital energy and separation $E_{\rm orb} \propto -1/a$, and ${\rm d}E_{\rm gw}/{\rm d}\omega = -{\rm d}E_{\rm orb}/{\rm d}\omega$, where $\omega = 2\pi f_{\rm orb} = \pi f$ is the orbital angular frequency of the binary, and a here is the semi-major axis of the elliptical orbit. Thus, loss of orbital energy is converted to GW energy emitted by a binary system.

3.4.4. *Cosmological sources*

Cosmological sources are associated with processes in the very early Universe, which take place well before the formation of stars and galaxies, see Fig. 3.6. The detection of cosmologically-generated GWs is a means for astronomers to observe the Universe mere fractions of a second after the Big

Bang, much earlier than what we can do with light. Currently, the earliest "picture" that we have of the universe is $\sim 380,000$ years after the Big Bang, when the Universe had cooled enough for neutral hydrogen atoms to form. This was the first time that photons could propagate freely, and those photons detected today constitute the cosmic microwave background (CMB) radiation. Fluctuation in the temperature of the CMB are associated with density perturbations in the Universe when it was roughly 1000 times hotter and 1000 times smaller than it is today. The potential detection of GWs produced by *inflation*, *first-order phase transitions*, and *cosmic strings* (discussed below) are three possible ways of probing much earlier in the evolution of the Universe.

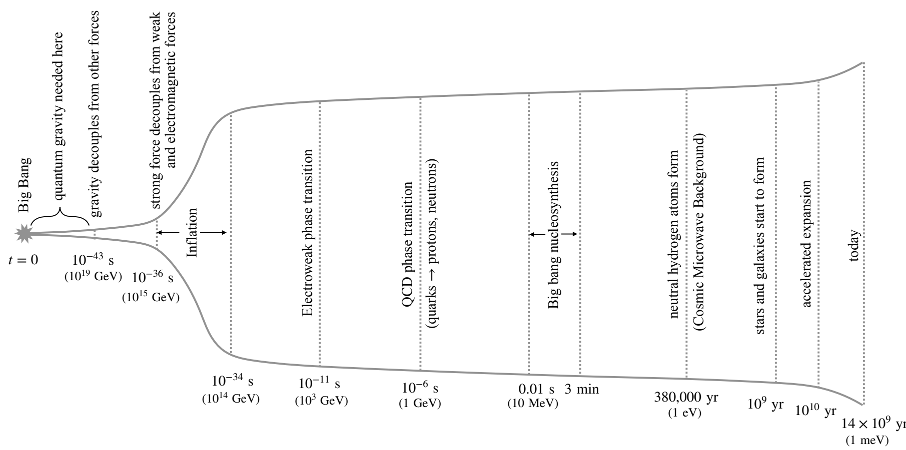

Figure 3.6: A schematic diagram showing the evolution of the Universe from the Big Bang until today, roughly 14 billion years laters. Highlighted are the times and energy scales for some important events during the history of the Universe.

Inflation: Inflation is the theory that the Universe experienced a period of rapid (exponential) expansion starting around 10^{-36} s after the Big Bang. This rapid expansion is thought to have stretched the Universe to macroscopic scales, making it incredibly smooth and flat. But quantum fluctuations in the vacuum energy density driving inflation would be amplified to macroscopic scales after inflation, becoming the "seeds" for the large-scale structure that we see today. Similarly, quantum fluctuations of the spacetime metric would also be amplified by inflation, leading to the production of GWs. These GWs would form a stochastic GW background that is essentially flat in energy density across the different frequency bands, see Fig. 3.7. Standard inflationary models would produce a background at the level of $\Omega_{\rm gw}(f) \sim 10^{-15}$ to 10^{-17} (constrained by the high level of isotropy of the CMB), which would be difficult to observe. However, there are modified theories of inflation which migh push the energy density to higher values at higher frequencies.

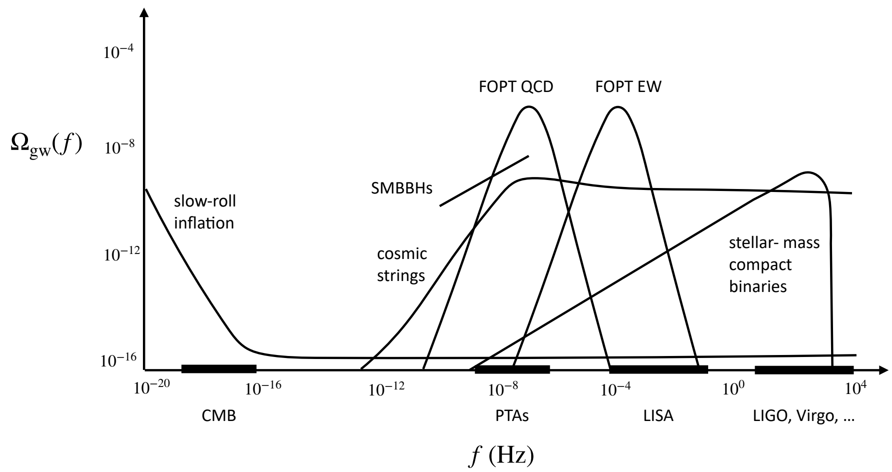

Figure 3.7: Representative energy density spectra for several different GW sources (both astrophysical and cosmological) across a large range of frequencies. The relevant frequency bands for different GW detectors are also shown.

First-order phase transitions (FOPTs): A first-order phase transition is associated with a discontinuity in certain thermodynamic properties of a material. For example, water boiling to produce steam is an example of a first order phase tranisition, since the entropy ($dS = dQ/T$) changes discontinuously with temperature due to the latent heat of vaporization at fixed $T = 100$ Celsius. In the same way that boiling water creates bubbles of the new phase (steam), which expand in the old phase (water) and collide with one another, creating sound waves and turbulent flows, so to would a first-order phase transition in the early universe create colliding bubbles and sound waves, which are the primary source of GWs.

Electroweak (EW) symmetry-breaking in the Standard Model is not thought to be a first-order phase transition. However, in some modifications to the Standard Model, a first-order phase transition might occur, producing GWs that could potentially be detected in the mHz frequency band (relevant for LISA). Similarly, a first-order QCD phase transition (when quarks first combine to form protons, neutrons, ...) would produce a stochastic GW background that is potentially observable by PTAs. Either of these observations would provide information about *new physics*, going beyond the predictions of the Standard Model (see Fig. 3.7).

Cosmic strings: Cosmic strings are one-dimensional topological defects, expected to form during phase transitions that have spontaneously broken symmetries. They are predicted in the context of grand unified theories. Cosmic strings would be relics of an earlier more-symmetric phase of the universe, decaying only via the emission of GWs. GWs are produced when the strings oscillate, form loops, cusps, and kinks, and interact with one another in a network of strings. Cosmic strings are usually quantified by the dimensionless string tension or mass-per-unit-length $G\mu/c^2$, where μ has dimensions of energy/length. A stochastic background of GWs from cosmic strings having $G\mu/c^2 \gtrsim 10^{-16}$ could be detectable with LISA.

3.5. Acknowledgments

JDR acknowledges financial support from National Science Foundation (NSF) Grant PHY-2207270, Physics Frontier Center Award PFC-2020265, as well as start-up funds from the University of Texas Rio Grande Valley. He also thanks colleagues Nelson Christensen and Marie-Anne Bizouard for their support and hospitality while visiting the Artemis Lab, Observatoire Cote D'Azur during the summer for the past several years.

3.6. Bibliography

Abbott, B. P., Abbott, R., Abbott, T. D., Abraham, S., Acernese, F., Ackley, K., Adams, C., Adhikari, R. X., Adya, V. B., Affeldt, C., et al. (2020), Gw190425: Observation of a compact binary coalescence with total mass $\sim 3.4\, m_{\odot}$, *The Astrophysical Journal Letters*, 892(1), L3. LIGO Scientific Collaboration and Virgo Collaboration.
URL: *https://doi.org/10.3847/2041-8213/ab75f5*

Abbott, B. P., Abbott, R., Abbott, T. D., Acernese, F., Ackley, K., Adams, C., Adams, T., Addesso, P., Adhikari, R. X., Adya, V. B., et al. (2017), GW170817: Observation of Gravitational Waves from a Binary Neutron Star Inspiral, *Physical Review Letters*, 119(16), 161101. LIGO Scientific Collaboration and Virgo Collaboration.
URL: *https://journals.aps.org/prl/abstract/10.1103/PhysRevLett.119.161101*

Abbott, B. P., Abbott, R., Abbott, T. D., et al. (2016), Observation of gravitational waves from a binary black hole merger, *Phys. Rev. Lett.*, 116, 061102.
URL: *https://link.aps.org/doi/10.1103/PhysRevLett.116.061102*

Allen, B. (1997), The stochastic gravity-wave background: Sources and detection, *in* J.-A. Marck, J.-P. Lasota, (eds), Relativistic Gravitation and Gravitational Radiation, vol. 26 of *Cambridge Contemporary Astrophysics*, Cambridge University Press, pp. 373–417.
URL: *https://arxiv.org/abs/gr-qc/9604033*

Allen, B., Romano, J. D. (2023), Hellings and Downs correlation of an arbitrary set of pulsars, *Phys. Rev. D*, 108, 043026.
URL: *https://link.aps.org/doi/10.1103/PhysRevD.108.043026*

Caprini, C., Figueroa, D. G. (2018), Cosmological backgrounds of gravitational waves, *Classical and Quantum Gravity*, 35(16), 163001.
URL: *https://dx.doi.org/10.1088/1361-6382/aac608*

Christensen, N. (2018), Stochastic gravitational wave backgrounds, *Reports on Progress in Physics*, 82(1), 016903.
URL: *https://dx.doi.org/10.1088/1361-6633/aae6b5*

Jenkins, A. (2021), Cosmology and Fundamental Physics in the Era of Gravitational-Wave Astronomy, Phd thesis, King's College London. Supervised by Mairi Sakellariadou.

Romano, J. D., Christensen, N. (2025), 'Stochastic gravitational wave backgrounds', `https://www.scholarpedia.org/article/Stochastic_gravitational_wave_backgrounds`. Scholarpedia article.